Catalysis Letters Vol. 107, Nos. 1–2, February 2006 (© 2006)
DOI: 10.1007/s10562-005-9732-z

An *in-situ* reduction/oxidation XAS study on the EL10V8 VO_x/TiO_2(anatase) powder catalyst

Geert Silversmit[a,*], Hilde Poelman[a], Isabelle Sack[b], Guy Buyle[a], Guy B. Marin[b], and Roger De Gryse[a]

[a]*Department Solid State Sciences, Ghent University, Krijgslaan 281 S1, B-9000 Gent, Belgium*
[b]*Laboratorium voor Petrochemische Techniek, Ghent University, Krijgslaan 281 S5, B-9000 Gent, Belgium*

Received 4 November 2005; accepted 24 November 2005

The structural changes of the supported vanadium oxide in the V_2O_5/TiO_2(anatase) EUROCAT EL10V8 powder catalyst during reduction and oxidation at 420 and 490 °C were studied with *in-situ* X-ray absorption spectroscopy (XAS). The Vanadium K-edge XAS results are compared with pure bulk V_2O_5. For the reduction–oxidation cycle at 420 °C, similar structural changes as for bulk V_2O_5 were observed for the supported vanadium oxide: a reduction to the VO_2 structure and re-oxidation back to V_2O_5. After reduction at 490 °C however, a different structure was obtained: very regular "VO_6" octahedra with a $V^{2.8+}$ valence. This may point to a structural support effect.

KEY WORDS: EUROCAT EL10V8; supported vanadium oxide; absorption spectroscopy; VO_x/TiO_2(anatase); *in-situ* XAS; V_2O_5.

1. Introduction

The European EUROCAT programme [1] consisted of a detailed study on two V_2O_5/TiO_2(anatase) powder catalysts with different V_2O_5 loadings (1 and 8 wt%). These catalysts were characterized with XRD, BET surface area, TPR, DTA, H_2 reduction and subsequent O_2 adsorption, vibration spectroscopies, NMR, EPR, XPS, SIMS, electric conductivity, chemical test reactions (partial oxidation of *o*-xylene to phthalic anhydride, decomposition of isopropanol),.... The two powders are therefore often used as reference catalyst systems.

X-ray absorption spectroscopy (XAS) was not applied in this EUROCAT study. As XAS can be performed *in-situ*, valuable structural information can be obtained with this technique. The present paper describes an *in-situ* VK-edge XAS study on the EUROCAT EL10V8 V_2O_5/TiO_2(anatase) powder catalyst (hereafter named V8) during two subsequent reduction/oxidation cycles at 420 and 490 °C. The XAS results are compared with pure unsupported V_2O_5 subjected to identical reduction/oxidation cycles at 420 °C.

An XAS experiment implies the registration of the total absorption of the sample as function of incident X-ray energy from ~200–100 eV before an absorption edge up to 1000 eV after the edge. The region around the absorption edge up to about 50 eV above it is called the XANES region (X-ray Absorption Near-Edge Structure) and the region beyond 50 eV above the edge the EXAFS region (Extended X-ray Absorption Edge Structure). This distinction is made as both regions contain different information: electronic information from the XANES region and structural from the EXAFS.

2. Experimental

The transmission Vanadium K-edge X-ray absorption spectroscopy (XAS) measurements were performed at the DUBBLE CRG beamline (BM26A) of the ESRF synchrotron during a 2*1/3 filling mode, giving a storage ring current of 200–160 mA. The XAS spectra were recorded with a Si(111) double crystal monochromator and ionisation chambers filled with Ar/He mixtures. The higher harmonics of the bending magnet synchrotron radiation that are also being transmitted by the monochromator were suppressed with the vertical focussing mirror after the monochromator.

Typically 5–6 mg of catalyst powder was mixed with 40 mg of BN, an inert and weakly absorbing binder, and pressed into the rectangular hole of a stainless steel sample holder. The weight of the sample was chosen to give a total absorption ($\mu x = \ln(I_0/I_t)$) of 2.5 at the Vanadium K-absorption edge in which I_0 is the intensity of the incident X-ray beam and I_t of the transmitted beam. For the *in-situ* measurements, a stainless steel XAS chemical cell designed and built at the Ghent University was used. The XAS cell has Kapton foils (25μm) as X-ray transparent windows. At the reaction temperatures, up to 6 spectra were averaged for the V8

* To whom correspondence should be addressed.

powder. The data quality was not sufficient to extract an EXAFS signal for this catalyst.

XAS spectra of V-foil, V_2O_5, VO_2, V_2O_3, VO, NH_4VO_3 and $VOSO_4{\cdot}3H_2O$ powders were recorded as references at ambient temperature in air. EXAFS data reduction and analysis were performed with the XDAP software [2]. The pre-edge background was subtracted using a modified Victoreen curve [3] and the atomic background, μ_0, was interpolated using a cubic spline routine [4]. The spectra were normalised by division of the absorption data by the value of the edge step at 50 eV above the edge position. The difference between the normalised spectra and μ_0 gives the EXAFS signal $\chi(k)$ where a transfer from energy to k-space is made$\left(k = \sqrt{\frac{2m_e}{\hbar^2}(h\nu - E_0)}\right)$, with E_0 the energy of the absorption edge and $h\nu$ the X-ray energy). A Fourier Transform (FT) of the EXAFS signal gives a pseudo radial distribution in R-space, usually $\chi(k)$ is multiplied with k^n (with $n=1$, 2 or 3) before taking the FT. The intensity of the pre-edge peak is calculated numerically as described previously [5], the error is estimated to be ± 0.1 (eV $\times$ normalised height).

The EL10V8 V_2O_5/TiO_2(anatase) powder is prepared via impregnation of the TiO_2-anatase support with vanadyl oxalate [1]. The V_2O_5(96%) powder was purchased from Merck, the VO_2 (99%) and V_6O_{13} (99.5%) powders were purchased from Alfa Aesar, the NH_4VO_3 (99.99%) and $VOSO_4{\cdot}3H_2O$ (99.99%) from Sigma Aldrich and the VO (99.5%) powder from Cerac.

An overview of the reduction/oxidation cycles at 420 °C applied to the V_2O_5 reference and the V8 catalyst is given in tables 1 and 2 respectively. Two reduction/oxidation cycles at 490 °C were also studied on the V8, the experimental conditions are summarized in table 3.

3. Results

First the XANES features of different V–O reference compounds are presented to illustrate what information can be obtained from V K XANES spectra (Section 3.1). Then the XANES and EXAFS results on the V_2O_5 reference powder are discussed (Section 3.2). Finally the XANES results on the V8 catalyst are compared with the V_2O_5 reference system (Section 3.3 and 3.4).

Table 1
History and experimental conditions applied to the V_2O_5 powder before and during X-ray absorption data collection for the reduction/oxidation cycles at 420 °C. RT stands for room temperature

Sample	Pre-treatment	Measuring conditions
1: V_2O_5(RT)	(a) 15 min 5% O_2/He flush,100 ml/min.	5% O_2/He, RT
2: V_2O_5(pre-OX)	(a) Treatment 1, (b) Heating from RT to 420 °C (10 °/min) in 5% O_2/He.	5% O_2/He, 420 °C
3: V_2O_5(RED)	(a) Treatment 2, (b) He flush, 1400 ml/min, 15 min, (c) 4 h reduction with 5% H_2/He (100 ml/min) at 420 °C.	5% H_2/He, 420 °C
4: V_2O_5(OX)	(a) Treatment 3, (b) He flush, 1400 ml/min, 15 min, (c) 1 h oxidation with 5% O_2/He at 420 °C.	5% O_2/He, 420 °C.

Table 2
History and experimental conditions applied to the V8 powder before and during X-ray absorption data collection for the reduction/oxidation cycles at 420 °C

Sample	Pre-treatment	Measuring conditions
1: V8(RT)	(a) 15 min 5% O_2/He flush at 400 ml/min; +40 min at 100 ml/min.	5% O_2/He, RT
2: V8(pre-OX)	(a) Treatment 1, (b) Heating from RT to 420 °C (10 °/min) in 5% O_2/He.	5% O_2/He, 420 °C
3: V8(RED1)	(a) Treatment 2, (b) He flush, 300 ml/min,10 min, (c) 1 h 16 min reduction with 5% H_2/He (100 ml/min) at 420 °C.	5% H_2/He, 420 °C
4: V8(OX1)	(a) Treatment 3, (b) He flush, 300 ml/min, 13 min, (c) 30 min oxidation with 5% O_2/He at 420 °C	5% O_2/He, 420 °C
5: V8(RED2)	(a) Treatment 4, (b) He flush, 300 ml/min,13 min, (c) 1 h 04 min reduction with 5% H_2/He (100 ml/min) at 420 °C	5% H_2/He, 420 °C
6: V8(OX2)	(a) Treatment 5, (b) He flush, 1400 ml/min, 15 min, (c) 1 h 16 min oxidation with 5% O_2/He at 420 °C.	5% O_2/He, 420 °C

Table 3
History and experimental conditions applied to the V8 powder before and during X-ray absorption data collection for the reduction/oxidation cycles at 490 °C

Sample	Pre-treatment	Measuring conditions
1: V8(RT)	(a) 15 min 5% O_2/He flush, 100 ml/min	5% O_2/He, RT
2: V8(pre-OX,490)	(a) Treatment 1, (b) Heating from RT to 490 °C (10 °/min) in 5% O_2/He.	5% O_2/He, 490 °C
3: V8(RED1,490)	(a) Treatment 2, (b) He flush, 300 ml/min, 10 min, (c) 4 h reduction with 100% H_2/He (100 ml/min) at 490 °C.	100% H_2, 490 °C
4: V8(OX1,490)	(a) Treatment 3, (b) He flush, 300 ml/min, 10 min, (c) 5 h oxidation with 5% O_2/He at 490 °C.	5% O_2/He, 490 °C
5: V8(RED2,490)	(a) Treatment 4, (b) He flush, 300 ml/min, 13 min, (c) 1 h 30 min reduction with 100% H_2/He (100 ml/min) at 460 °C.	100% H_2, 475–410 °C
6: V8(OX2,490)	(a) Treatment 5, (b) He flush, 1400 ml/min, 15 min, 460 °C (c) 1 h oxidation with 5% O_2/He at 460 °C.	5% O_2/He, 460 °C

3.1. V–O reference XANES spectra

The XANES spectra for different V–O reference compounds are given in figure 1 and some XANES characteristics are summarized in table 4. The energy scale is referenced to the offset (first maximum in derivative spectrum) of the Vanadium-foil spectrum, see [6]. Wong *et al*. [6] have performed an extensive study on the V K-edge XANES spectra of different vanadium compounds and showed that these spectra contain information on the vanadium oxidation state and the co-ordination symmetry around the V absorber. The position of the XANES features (pre-edge peak, main-edge, ...) shifts linearly towards higher energies with increasing vanadium cation valence. Most commonly the main-edge position is used to determine the vanadium valence. Our linear fit for the position of the absorption feature labelled 'A' in figure 1 ($1s \rightarrow 4p$ transition) as a function of vanadium oxidation state for pure vanadium oxides has smaller standard deviations than the corresponding fit for the main-edge positions. This makes the A position a better candidate for the vanadium oxidation state estimation, as also shown by Haaß *et al*. [7]. Figure 2 shows the energy shift in the A absorption feature for V_2O_5, VO_2, V_2O_3 and VO together with the linear fit (correlation factor of 0.999). From this linear relation, the vanadium valence of an unknown sample can be estimated with an error of ± 0.4.

Symmetrical vanadium–ligand co-ordinations with inversion symmetry, such as the regular "VO_6" octahedra in the VO and V_2O_3 structure, have only small pre-edge intensities. In contrast co-ordinations without inversion symmetry, like the distorted "VO_6" units in VO_2 and in $VOSO_4$ or the "VO_4" tetrahedrons in NH_4VO_3, have significant to large pre-edge intensities, see figure 1 and table 4.

3.2. V_2O_5

3.2.1. V_2O_5 redox cycle

The normalised XANES spectra for the different V_2O_5 treatments are given in figure 3, the XANES features are summarized in table 5 and the $k^{2*}\chi$ (k) spectra are shown in figure 4. After the measurement at room temperature (labelled V_2O_5(RT)), the V_2O_5 powder was heated to 420 °C in 5% O_2/He (V_2O_5(pre-OX)). The V_2O_5 structure remains and the XAS signals become less sharp due to the higher temperature.

After reduction with 5% H_2/He, the pre-edge peak intensity diminishes from 1.7 to 1.0 (V_2O_5(RED)). From comparison with the V–O reference XANES spectra it follows that distorted "VO_6" octahedra are present and the estimated valence is 4.2+. The $k^{2*}\chi(k)$ and

Table 4
XANES characteristics for selected V–O reference compounds. Energy positions relative to the offset of V-foil

Reference structure	Pre-edge peak position (eV)	Main-edge position (eV)	A position (eV)	Valence	Pre-edge peak intensity	V–O co-ordination
V_2O_5	5.5	16.1	29.6	5+	1.8	Distorted square pyramidal "VO_5" [8]
VO_2	4.9	12.8	26.4	4+	1.5	Distorted octahedral "VO_6" [9]
V_2O_3	–	10.4	23.3	3+	0.5	Regular octahedral "VO_6" [10]
VO	–	7.7	20.6	2+	–	Regular octahedral "VO_6" [11]
NH_4VO_3	5.1	17.5	27.2	5+	2.2	Tetrahedral "VO_4" [12]
$VOSO_4$	5.1	11.6	26.6	4+	0.8	Distorted octahedral "VO_6" [13]

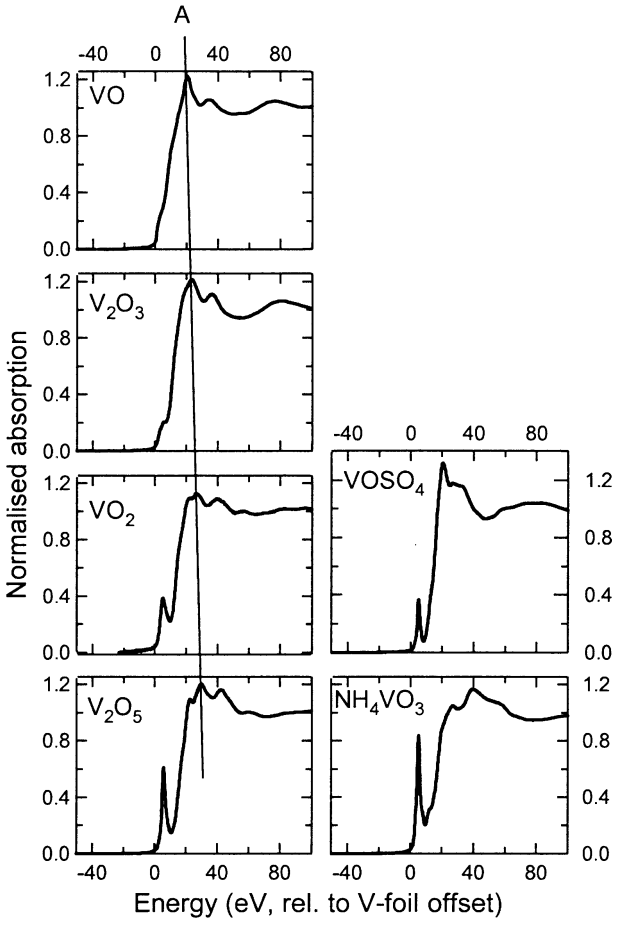

Figure 1. Normalised Vanadium K-edge XANES spectra for different V–O reference compounds.

FT[$k^{2*}\chi(k)$] spectra for V_2O_5(RED) are compared with the spectra for the VO_2 reference vanadium oxide in figure 5: there is very good agreement. Although there is some difference in magnitude for the V–V contribution

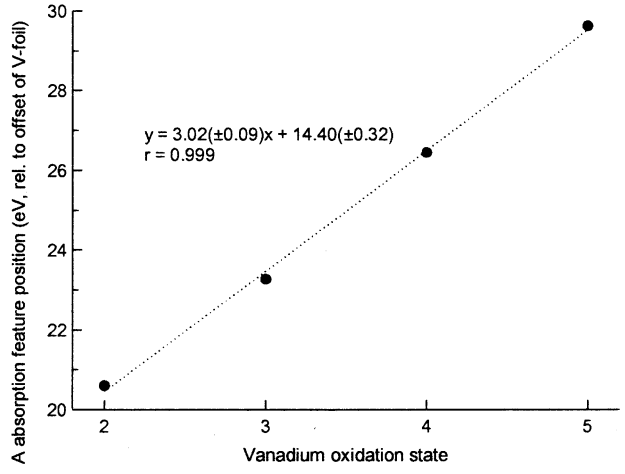

Figure 2. Position of the A absorption feature in the V K-edge XANES spectra from figure 1 for the pure vanadium oxides V_2O_5, VO_2, V_2O_3 and VO as a function of vanadium oxidation state. Energy positions relative to the offset of V-foil.

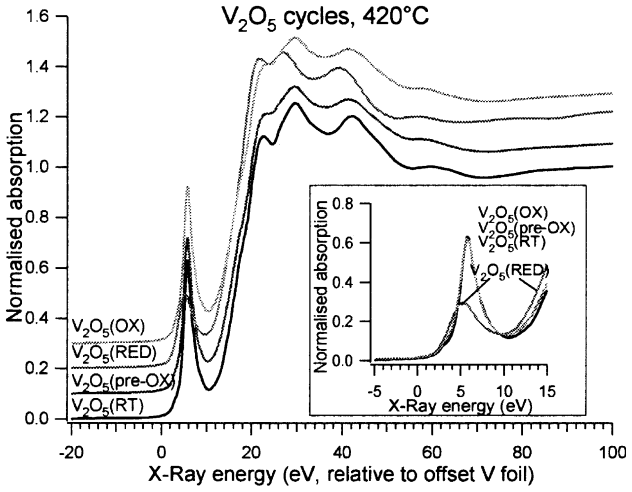

Figure 3. Normalised absorption spectra for the V_2O_5 treatments (for conditions, see table 1), spectra are shifted vertically for clarity. The inset shows the pre-edge region (without vertical shift).

around 3 Å, the imaginary part is identical, so a VO_2 structure can indeed be identified for V_2O_5(RED). The re-oxidation (V_2O_5(OX)) restores the V_2O_5 structure, see table 5, figures 3 and 4.

3.2.2. *The V_2O_5 reduction and re-oxidation process*

The spectra presented in the previous section were taken after full reaction, with the total reaction time given in the pre-treatment column in table 1. During the reduction and re-oxidation reaction full single scan XAS spectra were recorded to follow the reduction and re-oxidation. The evolution of the XANES spectra during reduction is given in figure 6 and the corresponding $k^{2*}\chi(k)$ spectra in figure 7. The pre-edge peak intensity diminishes continuously and the positions of the different XANES features shift to lower energy values. After 4 h reduction time no more changes were observed in the absorption spectra. The XANES and EXAFS spectra can be seen as a linear combination of the spectrum for V_2O_5(pre-OX) and V_2O_5(RED). The con-

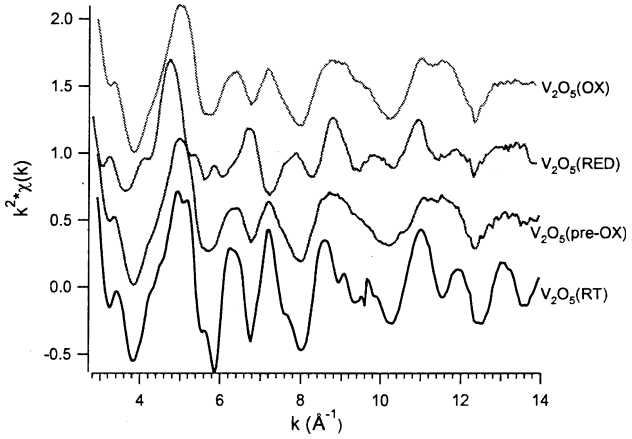

Figure 4. The $k^2\times\chi(k)$ EXAFS spectra for the V_2O_5 treatments (for conditions, see table 1), spectra are shifted vertically for clarity.

Table 5
XANES characteristics for the V_2O_5 treatments (for conditions, see table 1, energy positions relative to the offset of V-foil)

V_2O_5 treatment	Offset (eV)	Pre-edge peak position (eV)	Main-edge position (eV)	A (eV)	Estimated valence(± 0.4)	Pre-edge peak intensity	Estimated co-ordination
V_2O_5(RT)	4.9	5.7	15.9	29.3	4.9	1.7	As V_2O_5
V_2O_5(pre-OX)	4.9	5.7	15.8	31.0	4.9	1.7	As V_2O_5
V_2O_5(RED)	3.6	5.3	14.6	26.9	4.2	1.0	Distorted "VO_6"
V_2O_5(OX)	4.9	5.7	15.8	29.3	4.9	1.8	As V_2O_5

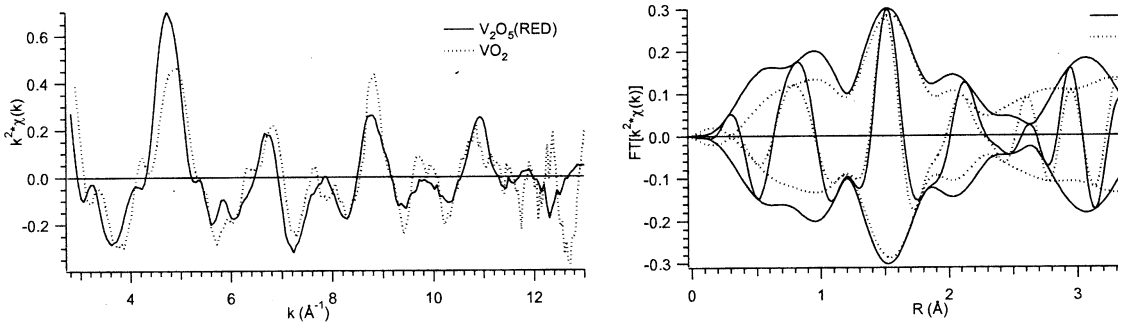

Figure 5. $k^2\times\chi(k)$ and FT[$k^2\times\chi(k)$] spectra for V_2O_5(RED) and VO_2 (ranges in k-space for the FT were 2.94–11.97 Å^{-1} (V_2O_5(RED)) and 3.08–12.45 Å^{-1} (VO_2)).

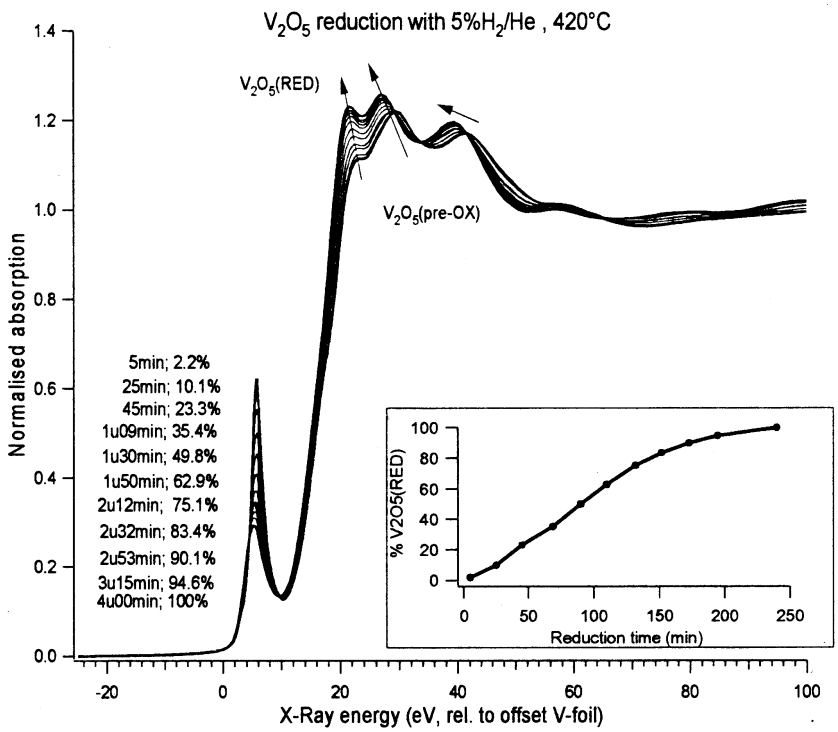

Figure 6. Normalised absorption spectra taken during the reduction of V_2O_5 (5% H_2/He, 420 °C). The total reduction time when each scan was started is indicated. Each spectrum can be seen as a linear combination of the spectrum for V_2O_5(pre-OX) and V_2O_5(RED). The percentages give the contribution of the V_2O_5(RED) spectrum and are given in the inset as function of reduction time.

tribution of the V_2O_5(RED) spectrum is indicated in figures 6 and 7 as percentage.

The evolution of the XANES spectra during the re-oxidation is given in figure 8 and the corresponding $k^{2*}\chi(k)$ spectra in figure 9. The pre-edge intensity increases and the positions of the different XANES features shift to higher energy values, until the V_2O_5 structure is obtained. The XANES and EXAFS spectra can be seen as a linear combination of the spectrum for V_2O_5(RED) and

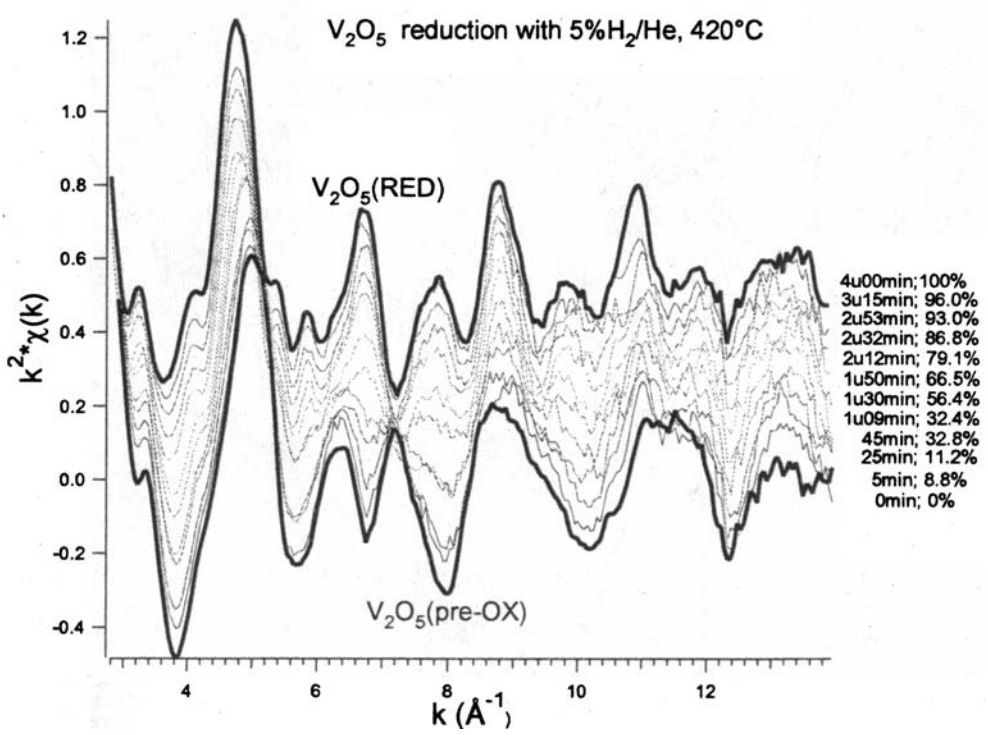

Figure 7. The $k^2 \times \chi(k)$ spectra taken during the reduction of V_2O_5 with 5% H_2/He at 420 °C. The total reduction time when each scan was started is indicated. Each spectrum can be seen as a linear combination of the spectrum for V_2O_5(pre-OX) and V_2O_5(RED). The percentages give the contribution of the V_2O_5(RED) spectrum, spectra are shifted vertically for clarity.

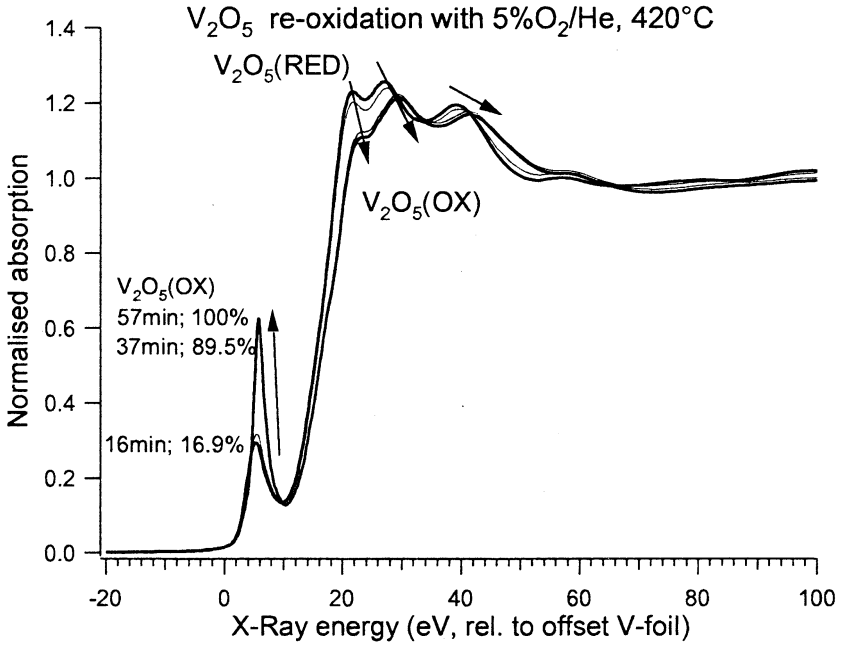

Figure 8. Normalised absorption spectra taken during the re-oxidation of V_2O_5(RED) with 5% O_2/He at 420 °C. The total re-oxidation time when each scan was started is indicated. Each spectrum can be seen as a linear combination of the spectrum for V_2O_5(RED) and V_2O_5(OX). The percentages give the contribution of the V_2O_5(OX) spectrum.

V_2O_5(OX). The contribution of the V_2O_5(OX) spectrum is indicated in figures 8 and 9. After 1 h re-oxidation time no more changes were observed. Hence, the re-oxidation is about 4 times faster than the reduction at 420 °C.

3.3. V8 at 420 °C

3.3.1. V8 redox cycle at 420 °C

The normalised absorption spectra for the V8 treatments at 420 °C are given in figure 10 and an overview

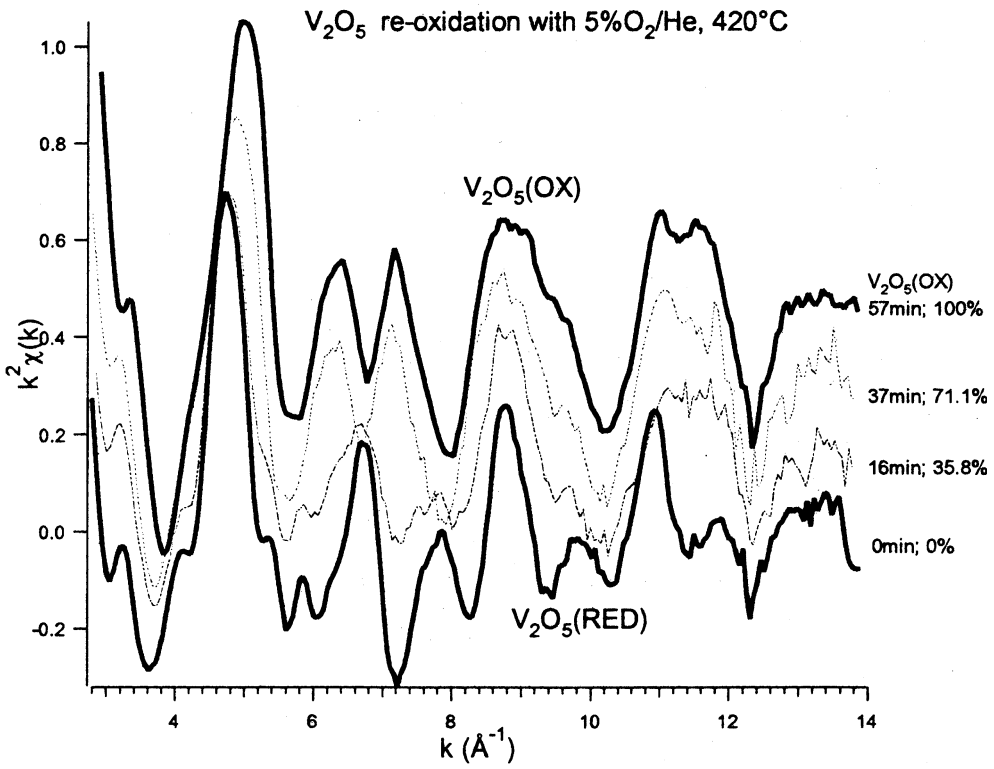

Figure 9. The $k^2 \times \chi(k)$ spectra taken during the re-oxidation of V_2O_5(RED) with 5% O_2/He at 420 °C. The total re-oxidation time when each scan was started is indicated. Each spectrum can be seen as a linear combination of the spectrum for V_2O_5(RED) and V_2O_5(OX). The percentages given the contribution of the V_2O_5(OX) spectrum, spectra are shifted vertically for clarity.

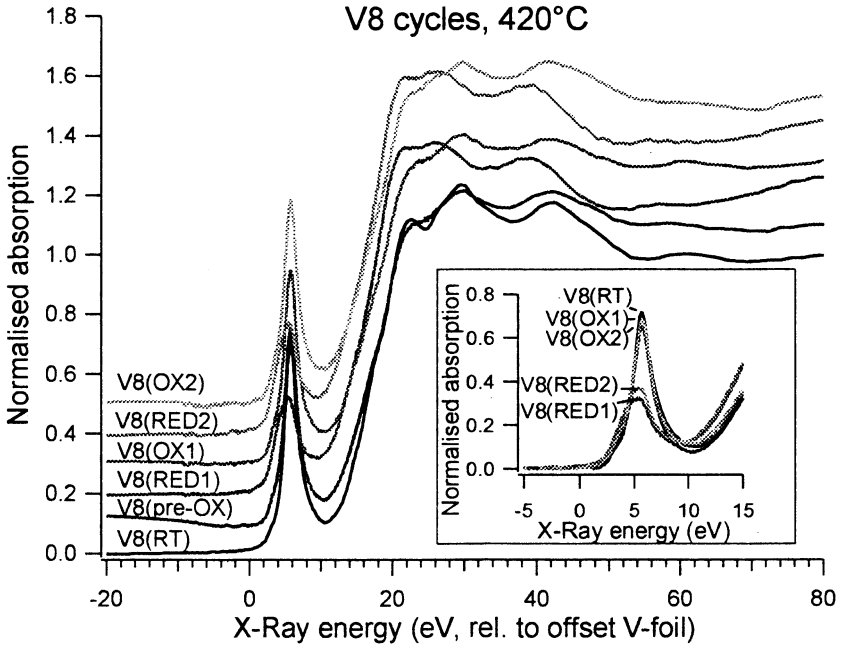

Figure 10. Normalised absorption spectra for the V8 treatments at 420 °C (for conditions, see table 2), spectra are shifted vertically for clarity. The inset shows the pre-edge region (without vertical shift).

of some XANES characteristics in table 6. Due to low vanadium amount only a small absorption signal was obtained (absorption step was 0.15), the data quality therefore did not allow to obtain an EXAFS spectrum.

At room temperature a clear V_2O_5 signal can be recognised in the XANES spectrum for V8(RT), see figure 10, with a vanadium valence and pre-edge peak intensity indeed similar to V_2O_5, see table 6. After heating the V8 catalyst to 420 °C in 5% O_2/He

Table 6
XANES characteristics for the V8 treatments at 420 °C (for conditions see table 2, energy positions relative to the offset of V-foil)

V8 treatment	Offset (eV)	Pre-edge position (eV)	Main-edge position (eV)	A (eV)	Estimated valence (±0.4)	Pre-edge peak intensity	Estimated co-ordination
V8(RT)	4.9	5.7	16.3	29.3	4.9	1.8	As V_2O_5
V8(pre-OX)	4.9	5.7	16.1	30.1	5.2	1.8	As V_2O_5
V8(RED1)	3.6	5.3	14.8	25.8	3.8	1.1	Distorted "VO_6"
V8(OX1)	4.9	5.7	15.8	29.3	5.2	1.8	As V_2O_5
V8(RED2)	3.4	5.5	14	30.1	4.0	1.3	Distorted "VO_6"
V8(OX2)	4.9	5.7	15.6	26.4	5.2	1.9	As V_2O_5

(V8(preOX)), the V_2O_5 structure remains, with only a weakening of the XANES signal due to the higher temperature.

Two successive reduction/oxidation cycles were performed on V8(preOX) at 420 °C. The reductions were performed with 5% H_2/He (V8(RED1) and V8(RED2)) and identical changes as for the V_2O_5 reference powder can be seen in the XANES spectra for both cycles. The pre-edge peak intensity diminishes to about 1.2 and the vanadium valence lowers to 4+. The supported vanadium oxide consists of distorted "VO_6" octahedra as in VO_2. The re-oxidations (V8(OX1) and V8(OX2)) bring back the V_2O_5 structure.

3.3.2. The V8 reduction and re-oxidation process at 420 °C

Figure 11 shows the normalised XANES spectra taken during the two reductions and re-oxidations at 420 °. As for the V_2O_5 reference powder, the re-oxidation process is faster than the reduction. No more changes are seen after about 20 min re-oxidation time about 1 h reduction time.

3.4. V8 at 490 °C

Two successive reduction/oxidation cycles were also performed on V8 at 490 °C, see table 3. The normalised XANES spectra are given in figure 12 and the XANES characteristics in table 7. In contrast to the cycles at 420 °C, the first reduction (V8(RED1,490)) has a different structure. There is only a very small pre-edge peak present, indicating that very regular "VO_6" octahedra are present in the supported vanadium oxide. The estimated vanadium oxidation state drops to 2.8+, a deeper reduction occurred.

Figure 13 compares the XANES spectrum for V8(RED1,490) with the one for V_2O_3. The past-edge structure is similar, but the shape of the pre-edge region is clearly different. Although the position of the A absorption feature is comparable, the main-edge for V8(RED1,490) has a higher energy. Again the V_2O_5 structure appears after re-oxidation.

The second reduction is similar to the reductions at 420 °C. The reaction temperature during this second reduction was however only 460 °C (see table 3), because the high temperature could not be maintained in the chemical XAS cell for long time. This may suggest that a higher reaction temperature is needed for the deeper reduction.

The stronger reduction of V8(RED1,490) was checked with a fast reduction/oxidation cycle at 490 °C. Figure 14 shows the single scan spectra after reduction and re-oxidation. The reduction time was 30 min in 100% H_2, performed on a new V8 sample previously heated in 5% O_2/He from room temperature to 490 °C. The reduction shows an identical spectrum as V8(RED1,490) from figure 12 with an estimated valence of 2.8+, confirming the deeper reduction.

4. Discussion

Two V_2O_5/TiO_2(anatase) powder catalysts with 1 or 8 wt% V_2O_5 loading (resp. V1 and V8) were extensively examined in the EUROCAT study [1]. Two vanadium oxide species were found in these supported vanadium oxide catalysts: vanadium oxide species in close contact with the TiO_2 support, probably present as mono-vanadates or poly-vanadates, and V_2O_5 crystallites, with larger V_2O_5 crystallites on V8. The V_2O_5 crystallites were observed on V8 with TEM en several diffraction peaks were found in the XRD patterns.

This XAS study on V8 shows indeed a V_2O_5 structure at room temperature and after all oxidation treatments. Moreover the supported vanadium oxide shows the same reduction/oxidation behaviour at 420 °C as bulk V_2O_5: a VO_2 structure after reduction and a V_2O_5 structure after re-oxidation. As all vanadium sites are probed with XAS, an average result is obtained, so the V_2O_5 crystallites dominate the XAS spectra. The possible mono- and poly-vanadates remain unnoticed.

The reductions at 490 °C yield a different structure for the supported vanadium oxide. The XANES spectrum has a weak pre-edge peak intensity, so very regular "VO_6" octahedra are present, with a 2.8+ vanadium oxidation state. The reductions at higher temperature were performed with 100% H_2, while the reduction at 420 °C was performed with 5% H_2/He. However we do not attribute the different structure to the difference in reaction gas composition. Since the reduction

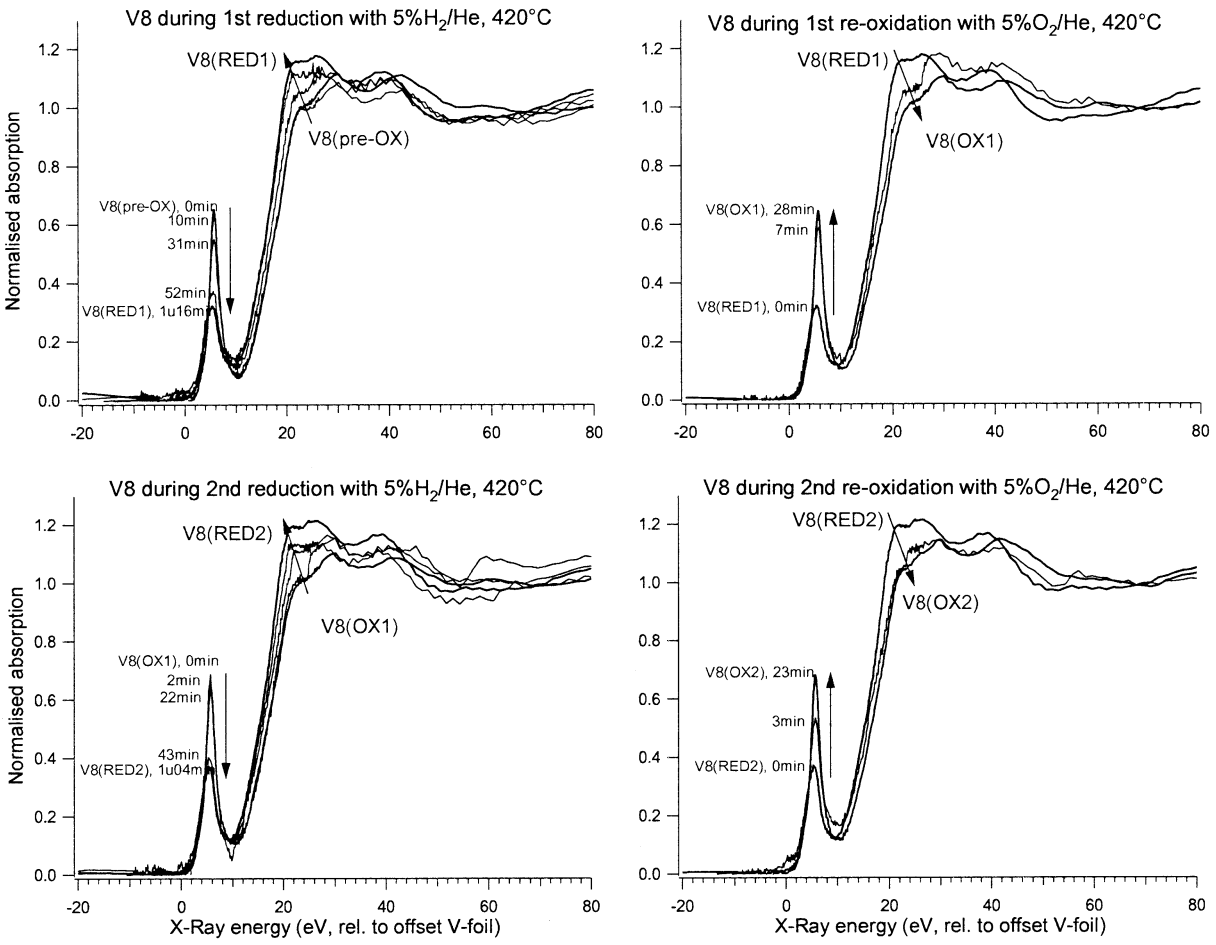

Figure 11. Normalised absorption spectra during the reduction of V8 (5% H_2/He, 420 °C). The total reduction time when each scan was started is indicated.

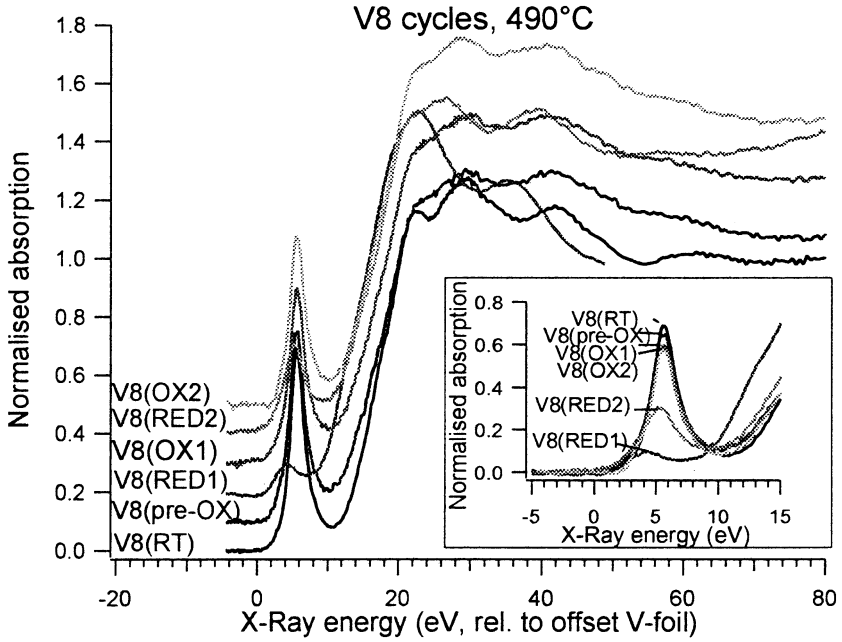

Figure 12. Normalised absorption spectra for the V8 treatments at 490 °C (for the experimental conditions, see table 3), spectra are shifted vertically for clarity. The inset shows the pre-edge region in more detail (without vertical shift).

Table 7
XANES characteristics for the V8 treatments at 490 °C (for the experimental conditions, see table 3), energy positions relative to the offset of V-foil

V8 treatment	Offset (eV)	Pre-edge position (eV)	Main-edge position (eV)	A (eV)	Estimated valence (±0.4)	Pre-edge peak intensity	Estimated co-ordination
V8(RT)	4.8	5.6	15.8	29.6	5.0	2.0	As V_2O_5
V8(pre-OX)	4.6	5.6	15.6	29.4	5.0	2.0	As V_2O_5
V8(RED1)	2.4	4.2	11.9	22.9	2.8	0.4	Very regular "VO_6"
V8(OX1)	4.6	5.6	16.2	30.2	5.2	1.8	As V_2O_5
V8(RED2)	4.0	5.4	13.4	26.7	4.1	1.1	Distorted "VO_6"
V8(OX2)	4.6	5.6	15.8	28.5	4.7	1.7	As V_2O_5

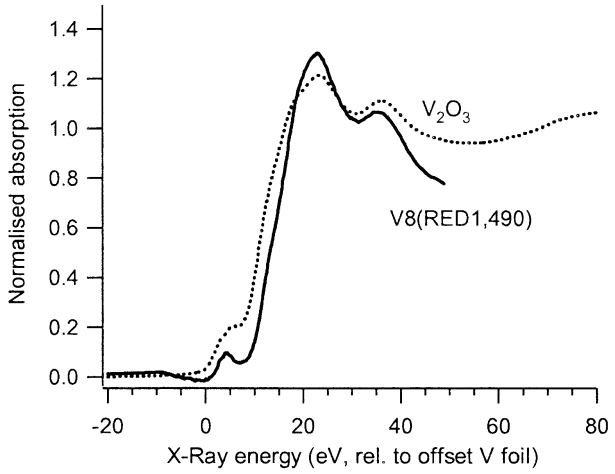

Figure 13. The XANES spectrum of V8(RED1,490) compared with V_2O_3.

V8(RED2,490) was performed with 100% H_2 at a reduction temperature of 460 °C and yielded an identical structure as V_2O_5(RED). The TPR (Temperature Programmed Reduction) profiles for V8 [1] show a maxima around 540 and 607 °C. Our reduction temperatures are thus below the first TPR maximum, so the same reaction mechanism can be assumed for the two reduction temperatures.

Although the post-edge structure of the XANES spectra for V8(RED1,490) has good agreement with V_2O_3, the shape of the pre-edge peak is clearly different, the pre-edge peak is more isolated from the main edge and its main-edge has a higher energy value, see figure 13. We have observed a similar XANES spectrum on an industrial VO_x/TiO_2(anatase) catalyst that was reduced at 350 °C with 5% H_2/He after heating in inert atmosphere [5]. The EXAFS analysis on that catalyst showed very regular "$V^{<4+}O_6$" octahedra with four V–O bonds of 1.9 Å, two V–O bonds of 2.1 Å and V–M bonds at 3.1 Å (with M = V or Ti), bond distances comparable to the interatomic distances in TiO_2. The V–M distances do not correspond to the V–V bond distances in V_2O_3 which are 2.70 and 2.88 Å [10]. Therefore a structural support effect was proposed for this industrial VO_x/TiO_2(anatase) catalyst, as the supported vanadium oxide had a structure different from known vanadium oxide compounds. The TiO_2 support possibly stabilizes the supported vanadium oxide in a structure not accessible in the known vanadium oxide compounds [5]. A Vanadium site symmetry similar to that of Ti sites in TiO_2 was recently also observed with XAS by Izumi *et al.* [14] on vanadium oxide supported on TiO_2 powder (Degussa P25) after reaction with isopropanol. As for V8(RED1,490), a weak isolated pre-edge peak and an intense $1s \rightarrow 4p$ transition is visible in the XANES spectra of Izumi *et al.* [14].

A local vanadium co-ordination similar to the Ti co-ordination in TiO_2 can thus be assumed for V8(RED1,490). A structural support effect can be responsible for this structure.

5. Conclusions

X-ray absorption spectroscopy was not included in the European EUROCAT study on the 1 and 8 wt% V_2O_5/TiO_2(anatase) catalysts. The presented XANES study on the 8 wt% V_2O_5/TiO_2(anatase) V8 catalyst provides therefore supplementary information to the EUROCAT programme.

The calcined V8 catalyst has a V_2O_5 XANES signal. The supported vanadium oxide in V8 shows identical structural changes as bulk V_2O_5 during reduction and oxidation at 420 °C with 5% H_2/He and 5% O_2/He respectively. A VO_2 structure is obtained after reduction and the V_2O_5 structure reappears after re-oxidation. However, when the reduction is performed at 490 °C, a different structure is observed: very regular "VO_6" octahedra are present with a 2.8+ (±0.4) vanadium oxidation state. From comparison with previous results on an industrial VO_x/TiO_2(anatase) powder, this may point to a structural support effect, where the TiO_2 support stabilizes the supported vanadium oxide in a structure not accessible for the known vanadium oxide compounds.

Acknowledgments

We acknowledge the European Synchrotron Radiation Facility for provision of synchrotron radiation facilities and we would like to thank Sergey Nikitenko

Table 8
XANES characteristics for the V8 XANES spectra from figure 14, fast cycle at 490 °C

V8 treatment	Offset (eV)	Pre-edge peak position (eV)	Main-edge position (eV)	A (eV)	Estimated valence (±0.4)	Pre-edge peak intensity	Estimated co-ordination
V8(RED)	2.2	4.2	11.1	22.9	2.8	0.5	Very regular "VO_6"
V8(OX)	4.6	5.6	15.0	29.4	5.0	1.9	As V_2O_5

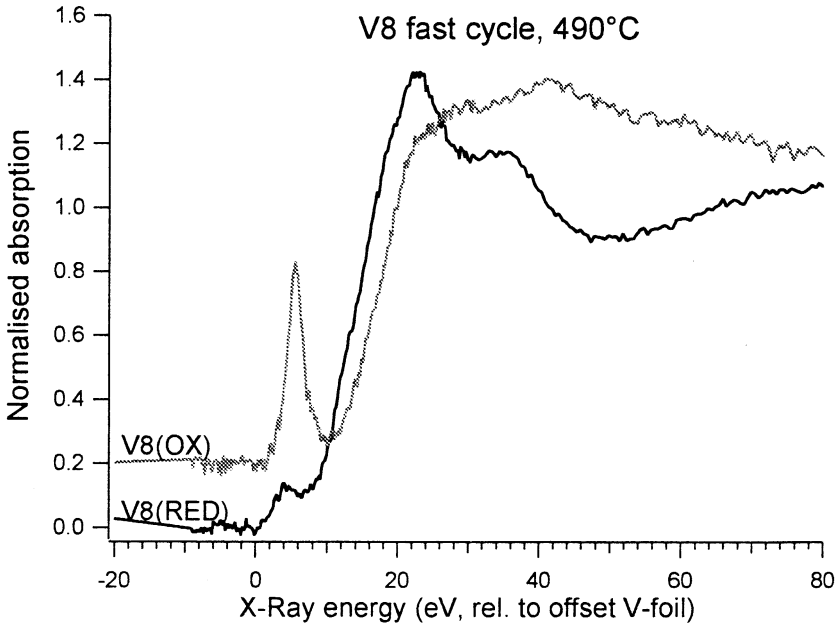

Figure 14. Normalised XANES spectra for the fast reduction/oxidation cycle on the V8 catalyst at 490 °C, spectra are shifted vertically for clarity.

for assistance in using the XAS station at the DUBBLE beamline (BM26A). This work was performed as part of a project of the Fund for Scientific Research, Flanders (FWO-Vlaanderen), in the framework of the Belgian Programme on Interuniversity Poles of Attraction initiated by the Belgian State, Prime Minister's Office, Science Policy Programming (IUAP-V/03) and of a Concerted Research Action (GOA) financed by the Ghent University. Its authors assume the scientific responsibility.

References

[1] J.C. Védrine, (ed) EUROCAT, Catal. Today 20 (1994) 1.
[2] M. Vaarkamp, J.C. Linders and D.C. Koningsberger, Physica B 208 & 209 (1995) 159.
[3] M. Vaarkamp, I. Dring, R.J. Oldman, E.A. Stern and D.C. Koningsberger, Phys. Rev. B 50 (1994) 7872.
[4] J.W. Cook Jr. and D.E. Sayers, J. Appl. Phys. 52 (1994) 5024.
[5] G. Silversmit, J.A. van Bokhoven, H. Poelman, A.M.J. van der Eerden, G.B. Marin, M-F Reyniers and R. De Gryse, Appl. Catal. A 285 (2005) 151.
[6] J. Wong, F.W. Lytle, R.P. Messmer and D.H. Maylotte, Phys. Rev. B 30 (1984) 5596.
[7] F. Haaß, A.H. Adams, T. Buhrmester, G. Schimanke, M. Martin and H. Fuess, Phys. Chem. Chem. Phys. 5 (2003) 4317.
[8] H.G. Barnes, F.R. Ahmed and W.H. Barnes, Z. Kristallogr. 115 (1961) 110.
[9] J.M. Longo and P. Kierkegaard, Acta Chem. Scand. 24 (1970) 420.
[10] M.G. Vincent, K. Yvon and J. Ashkenazi, Acta Cryst. A 36 (1980) 808.
[11] N. Schönberg, Acta Chem. Scand. 8 (1954) 221.
[12] H.T. Evans Jr., Z. Kristallogr. 114 (1960) 257.
[13] F. Théobald and J. Galy, Acta Cryst. B 29 (1973) 2732.
[14] Y. Izumi, F. Kiyotaki, N. Yagi, A-M. Vlaicu, A. Nisawa, S. Fukushima, H. Yoshitake and Y. Iwasawa, J. Phys. Chem. B 109 (2005) 14884.